

Propofol-induced apoptosis of neurones and oligodendrocytes in fetal and neonatal rhesus macaque brain

C. Creeley¹, K. Dikranian², G. Dissen³, L. Martin³, J. Olney¹ and A. Brambrink^{3,4*}

¹ Departments of Psychiatry and ² Anatomy and Neurobiology, Washington University School of Medicine, St Louis, MO, USA

³ Division of Neuroscience, Oregon National Primate Research Center, OR, USA

⁴ The Department of Anesthesiology and Perioperative Medicine, Oregon Health and Science University, Portland, OR, USA

* Corresponding author. E-mail: brambrin@ohsu.edu

Editor's key points

- Exposure of fetal or neonatal non-human primates to ketamine or isoflurane anaesthesia causes widespread apoptosis.
- The effects of propofol were compared using the same NHP model.
- Propofol caused a similar pattern of apoptosis of neurones and oligodendrocytes as isoflurane.
- Propofol, compared to isoflurane, induces apoptosis of less magnitude in both fetal and neonatal brain.

Background. Exposure of the fetal or neonatal non-human primate (NHP) brain to isoflurane or ketamine for 5 h causes widespread apoptotic degeneration of neurones, and exposure to isoflurane also causes apoptotic degeneration of oligodendrocytes (OLs). The present study explored the apoptogenic potential of propofol in the fetal and neonatal NHP brain.

Method. Fetal rhesus macaques at gestational age 120 days were exposed *in utero*, or postnatal day 6 rhesus neonates were exposed directly for 5 h to propofol anaesthesia ($n=4$ fetuses; and $n=4$ neonates) or to no anaesthesia ($n=4$ fetuses; $n=5$ neonates), and the brains were systematically evaluated 3 h later for evidence of apoptotic degeneration of neurones or glia.

Results. Exposure of fetal or neonatal NHP brain to propofol caused a significant increase in apoptosis of neurones, and of OLs at a stage when OLs were just beginning to myelinate axons. Apoptotic degeneration affected similar brain regions but to a lesser extent than we previously described after isoflurane. The number of OLs affected by propofol was approximately equal to the number of neurones affected at both developmental ages. In the fetus, neuroapoptosis affected particularly subcortical and caudal regions, while in the neonate injury involved neocortical regions in a distinct laminar pattern and caudal brain regions were less affected.

Conclusions. Propofol anaesthesia for 5 h caused death of neurones and OLs in both the fetal and neonatal NHP brain. OLs become vulnerable to the apoptogenic action of propofol when they are beginning to achieve myelination competence.

Keywords: anaesthetics *i.v.*, propofol; developing brain; neurones; non-human primates; oligodendroglia; toxicity

Accepted for publication: 6 April 2013

Anaesthetic drugs cause widespread apoptotic neurodegeneration in the developing brains of several animal species,^{1–7} including non-human primates (NHPs),^{8–12} and neonatal exposure to these agents is associated with long-term neurobehavioural disturbances in both rodents^{2,4,5,13} and NHPs.¹⁴ There is also recent evidence for a significant association between exposure of human infants to brief anaesthesia and risk for long-term neurobehavioural impairment.^{15–21} There is also evidence^{22,23} that isoflurane exposure of infant rhesus macaques causes glial cells of the oligodendrocyte (OL) lineage to undergo apoptosis, and these cells become vulnerable at a time when they are just beginning to myelinate axons that interconnect neurones throughout the central nervous system.

Prior research documents neuroapoptosis induced in the fetal and neonatal and NHP brain by isoflurane^{10,11} or ketamine^{8,9,12} and, most recently, apoptosis of OLs in the fetal and neonatal NHP brain by isoflurane.^{22–24} Propofol is used widely in paediatric patients to provide deep sedation/

anaesthesia for surgery, and diagnostic or therapeutic procedures. In the infant rodent brain propofol induces neuroapoptosis,⁷ but it is unknown whether propofol has similar toxic properties in the developing NHP brain. Therefore, we conducted a series of experiments to determine the apoptogenic action of propofol on the developing NHP brain at 120 days gestation (G120, full term=165 days), or at postnatal day 6 (P6).

Methods

Animals and experimental procedures

All animal procedures were approved by the Oregon National Primate Research Center and Washington University Medical School Institutional Animal Care and Use Committees, and were conducted in full accordance with the PHS Policy on Humane Care and Use of Laboratory Animals. Propofol anaesthesia was administered to the experimental animals after the same standard of care that is practiced in a state-of-the-art

operating room as described by the American Society of Anesthesiologists. All animals were tracheally intubated, mechanically ventilated and monitored for physiologic homeostasis throughout the experiment. An abbreviated description of these methods is given below, and a more detailed description is presented in the Appendix (see Supplementary material).

Rhesus macaques were studied at a fetal age of G120 (corresponds in brain age to that of a late third-trimester human fetus), or at a neonatal age of P6 (corresponds to brain age of a 4–6-month-old human infant). The experimental fetuses ($n=4$) were exposed *in utero*, and the experimental infants ($n=4$) were exposed directly, for 5 h to propofol as the sole anaesthetic agent. In all cases (dams and infants), the anaesthetic was titrated to provide a moderate plane of surgical anaesthesia (no movement and not >10% increase in heart rate or arterial pressure in response to a mosquito-clamp pinch at hand and foot; checked every 30 min). This type of response to standardized deep skin stimulation is typical for a level of anaesthesia that would be adequate for skin incision and the initiation of surgery.

The G120 fetuses were bred in a time-mated manner for these experiments, and the assigned dams were not exposed to any sedative agents during pregnancy. At G120, the pregnant dams were exposed for 5 h to an i.v. infusion of propofol ($n=4$), or to no anaesthesia ($n=4$, control). After propofol was discontinued, the dams awakened within 15 min were extubated and further observed for 3 h at which time a Caesarean section was performed under propofol anaesthesia. In order to obtain the fetal brain for histopathological analysis, the fetus received a coma-inducing dose of pentobarbital immediately after delivery and was euthanized by perfusion fixation according to relevant NIH guidelines.

The P6 infants were exposed for 5 h either to propofol ($n=4$) or no anaesthesia ($n=5$; controls). The infants were naturally delivered from dams that had been group housed or were part of the time-mated breeding programme. After propofol anaesthesia was discontinued at 5 h, the infants awakened and were extubated when fully awake and observed for 3 h in an animal incubator. At the end of the observation period, physiologic data were recorded, the infants were given high-dose pentobarbital and were euthanized by transcardial perfusion-fixation in keeping with National Institutes of Health (NIH) guidelines.

The control dams for the fetal study remained in their home cages until Caesarean section for delivery of the fetus at 8 h after time zero and each control fetus was handled exactly as described for the propofol-exposed animals. The control infants were subjected to venipuncture for blood sampling, physiological monitoring and to receive an injection of saline, and were then returned to their mothers until euthanasia at 8 h from time zero.

Histopathology

To assess the effects of propofol on both neurones and glia we adopted the following basic protocol: after *in vivo* perfusion

fixation with 4% paraformaldehyde, 70 μ M serial sections were cut on a vibratome across the entire rostro-caudal extent of the forebrain, midbrain, brainstem and cerebellum. Four series of adjacent sections were selected at 2 mm intervals across the entire brain. The first series was stained by activated caspase 3 (AC3) immunocytochemistry (ICC), which is a marker for apoptosis and stains both cell bodies and processes of neurones or glia in the very early and relatively late stages of apoptosis.^{11 12} The second series was stained by the DeOlmos cupric silver method, which stains all cells that are dead or dying.^{1 2} The third series was stained with antibodies against fractin, which is a breakdown product that is generated by caspase-mediated proteolysis of actin in cells that are undergoing apoptosis.^{24 25} The fourth series was stained by myelin basic protein (MBP) ICC, a method for visualizing young, differentiated OLs that are preparing to engage, or are already engaged in myelination.^{24 26 27}

To further evaluate the type and maturational state of cells that undergo apoptosis after propofol exposure, we used immunofluorescent double staining for AC3 or fractin (markers for apoptosis) and glial fibrillary acidic protein (GFAP; marker for astrocytes), Iba1 (marker for microglia and macrophages), platelet-derived growth factor receptor alpha (PDGFR α ; marker for OL progenitors), MBP (marker for premyelinating and myelinating differentiated OLs), or NeuN (marker for mature neurones). In all of the double staining immunofluorescent experiments we counterstained with 4',6-diamidino-2-phenylindole (DAPI), a stain that detects abnormal changes in nuclear chromatin pattern indicative of apoptotic cell death. Regions of interest were viewed and digital images were obtained using a Leica DFC310 Microsystems fluorescence microscope (North Central Instruments, Inc., Plymouth, MN, USA) operated by Leica Application Suite software. The staining protocols modelled those previously published^{22 24} and are further detailed in the Appendix (see Supplementary material).

Quantification of apoptosis

AC3-positive neuronal profiles were counted by an investigator who was blinded to the treatment condition. The counts were performed on sections selected in an unbiased manner at 2 mm intervals from serial sections cut across the entire brain. Each stained section was analysed by light microscopy using a 10 \times objective lens and a computer-assisted Stereo Investigator system (MicroBrightfield, Inc., Williston, VT, USA) with an electronically driven motorized stage. In each section, the identity and location of each AC3 stained profile was plotted. The rater used colour-coding and, on the basis of location and morphological appearance, plotted each stained profile as either a red dot (neurone) or white dot (glia). The total area scanned and the total number of stained neurones or glia per section and per brain were computer-recorded. From the recorded information, the density of apoptotic profiles per cubic millimetre was estimated for the entire brain or for any given region within the brain, and the total number of apoptotic profiles in the entire brain was also estimated. In addition, a computer plot showing the regional distribution of stained

profiles was generated and the plots for each region of each brain for each treatment condition were compared. These AC3 counts were used to compare the magnitude of apoptotic degeneration of neurones and glia in the control and propofol-exposed brains.

Statistical analysis

Data are presented as mean [standard error of the mean (SEM)], except for physiologic variables that are provided as median and range. Student's *t*-test with Welch correction, where appropriate, was used. A two-sided *P*-value of <0.05 was judged significant, and the 95% confidence interval (CI) for the mean difference provided a measure of precision. Statistical analysis was performed with Prism GraphPad Software, Inc. (San Diego, CA, USA).

Results

Fetal response to propofol

The pregnant dams randomized to this study received propofol anaesthesia or no anaesthesia (control) on post-conception day 120 (1) days [mean (SEM); range 117–124]. The 'propofol' group ($n=4$; body weight 7.4–8.8 kg) maintained physiologic homeostasis throughout the experiment (Supplementary Table S1). No adverse effects of propofol administration were observed and the pregnant animals recovered quickly (<15 min) without evidence of post-anaesthesia complications. Caesarean section 3 h later was well tolerated as documented by maternal and fetal vital signs within normal limits (Supplementary Table S2). The 'control' group ('no anaesthesia'; $n=4$; body weight 5.4–7.5 kg) received general anaesthesia only for the Caesarean section and their vital signs were comparable with those of the 'propofol' group (Supplementary

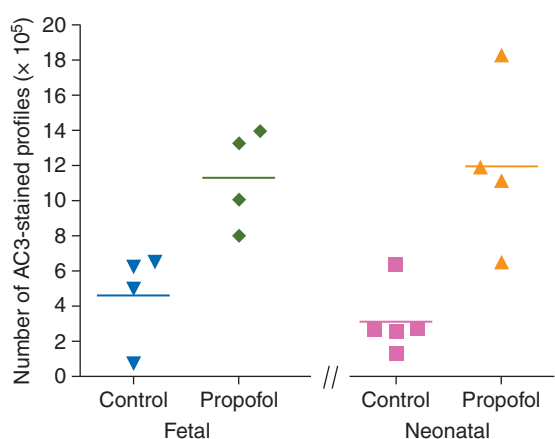


Fig 1 The total number of profiles (neurones+glia) undergoing apoptosis, as determined by AC3 staining, in fetal or neonatal NHP brain after exposure to propofol or to no drug (control). The difference between the mean apoptosis counts for propofol-exposed or control brain at each age was statistically significant (fetuses $P=0.01$; neonates $P=0.007$).

Table S2). Fetal body weights (propofol group 206–274 g; control group 129–252 g), and other standard body dimensions were age-appropriate for the macaque G120 time point and did not differ between experimental groups. No complications occurred during *in-vivo* perfusion fixation of the fetuses.

Quantitative findings

Quantitative evaluation of AC3-stained sections from the fetal brains exposed to propofol ($n=4$) revealed that the mean (SEM) number of all AC3-positive profiles (neurones+glia) per brain was 11.3 (1.4), and in the control brains ($n=4$) was 4.6 (1.3) (Fig. 1). Hence, there was a 2.4-fold increase in the number of apoptotic profiles in the propofol-exposed brains compared with the brains from drug-naïve controls. The difference in the mean number of apoptotic profiles between the propofol and control groups was 6.7×10^5 (95% CI, $11.4 \times 10^5 - 2.0 \times 10^5$, $P=0.01$). In the fetal NHP brains exposed to propofol, the mean number of dying (AC3-positive) neurones was approximately equal to the mean number of AC3-positive OLs (5.69×10^5 for neurones and 5.63×10^5 for OLs).

Descriptive histopathology

The regional distribution of cells undergoing acute apoptotic degeneration, as assessed by AC3 staining, in the G120 NHP fetal brain at a representative mid-rostrocaudal level after exposure to propofol or 'no anaesthesia' (control) is illustrated in Figure 2.

Neuronal degeneration in the propofol-exposed brains was distributed evenly and in moderate density across several

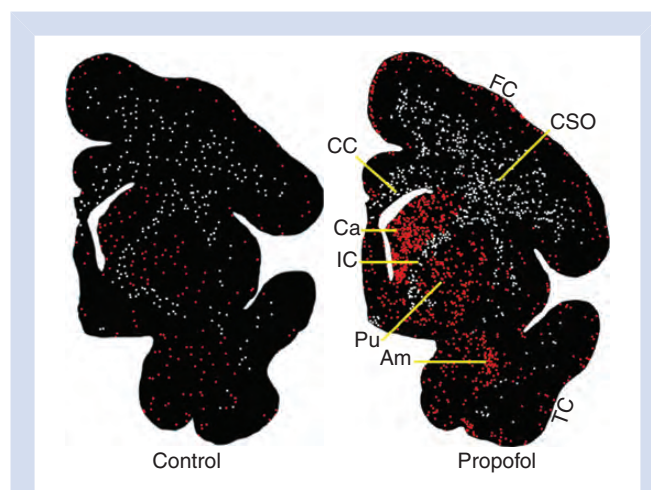


Fig 2 Computer plots showing the pattern of apoptotic cell loss in representative sections from a mid-rostrocaudal level of control or propofol-exposed fetal NHP brains. Apoptotic neurones (red dots) and apoptotic OLs (white dots) are more abundant in the propofol-exposed than control brain. Apoptotic neurones are most densely concentrated in several layers of the frontal cortices and temporal cortices, the caudate (Ca) nucleus, putamen (Pu), amygdala (Am), and in caudal regions not shown here (cerebellum and inferior colliculus). Apoptotic OLs are diffusely distributed throughout WM regions, including the centrum semi-ovale (CSO), corpus callosum (CC), and internal capsule (IC).

divisions (frontal, parietal, and temporal) of the neocortex. The majority of cerebrocortical degenerating neurones were pyramidal shaped, had prominent apical dendrites and were distributed in cortical Layers II to IV (Fig. 3). Degenerating neurones were present in very high density in the caudate

nucleus, putamen and nucleus accumbens, and in moderately high density in the amygdala and thalamus. The majority of degenerating neurones in the caudate nucleus and putamen had oval-shaped, medium sized cell bodies and morphologically resembled immature spiny stellate neurones of the type that comprise >90% of cells in the caudate and putamen. There also were infrequent larger degenerating profiles, which morphologically resembled cholinergic neurones that are large in size and comprise ~1% of the neuronal population in the caudate/putamen. In previous studies pertaining to neuroapoptosis induced in the fetal NHP brain by isoflurane,²⁴ ketamine,¹² or alcohol,²⁸ we have observed that these same neuronal populations in the caudate and putamen are selectively vulnerable. At the cerebellar-brainstem level, the highest density of degenerating neurones was in the internal granule cell layer of the cerebellum and in the inferior colliculus. This distribution of neuronal degeneration in both rostral and caudal brain regions closely resembles what we recently described^{23 24} in the G120 fetal NHP brain after isoflurane exposure.

Degenerating glial profiles visualized by AC3 staining in the propofol-exposed fetal brains were distributed diffusely throughout the white matter (WM) at all levels of the neuraxis, and the distribution pattern conformed to the location of specific WM pathways at each level (see Fig. 2). We stained sections adjacent to the AC3-stained sections with the DeOlmos cupric silver method (marker for dying cells), and with antibodies to fractin (marker of caspase-mediated proteolytic degradation), and observed that these stains marked approximately the same number of cells in the same WM locations as were marked by AC3, and the cells stained by silver or fractin were similar in morphological appearance to those stained by AC3 (Fig. 4A–C). While fractin and AC3 appeared to stain the same population of dying cells in the WM, fractin did not detect dying cells in various grey matter regions where AC3 vividly

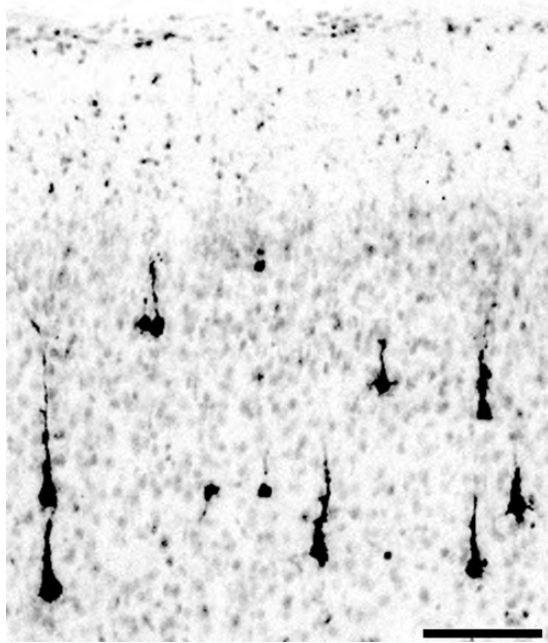


Fig 3 Histological appearance of degenerating neurones, as revealed by AC3 staining, in the frontal cortex of the NHP fetus after 5 h of propofol anaesthesia. The affected neurones are pyramidal, have a prominent apical dendrite and are distributed evenly across Layers II, III, and IV. Scale bar=50 μ m.

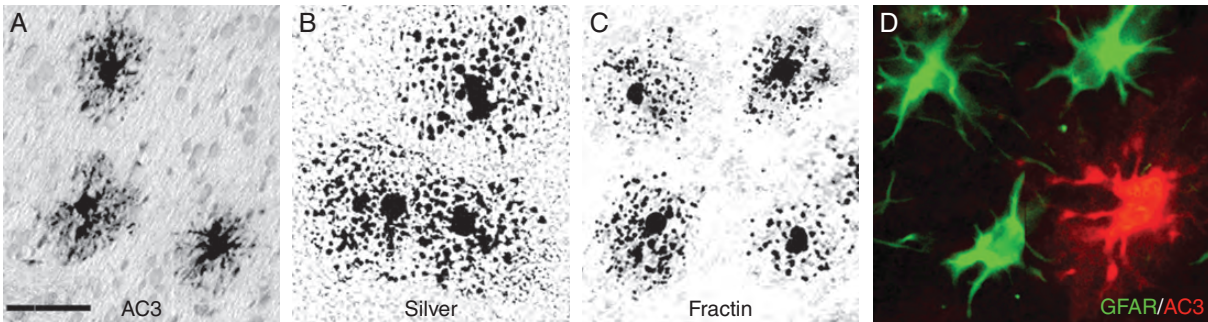


Fig 4 Morphological and staining characteristics of degenerating glia in the centrum semi-ovale WM underlying the frontal cortex of a propofol-exposed fetal NHP brain. AC3 staining (A) displays the degenerating OLs as spider-like profiles surrounded by a smudgy halo comprised of disintegrating processes and perhaps AC3 protein that has leaked out of the cell. Silver staining (B) displays the cell body and a starburst pattern of fragmented debris shed by the degenerating processes. Fractin antibodies (C) detect fractin, a breakdown product formed by proteolysis of actin, which is present throughout the cell body and processes of OLs. Each of these cell death markers detects degenerating OLs in approximately the same numbers and distribution throughout the WM. (D) A section immunofluorescently double stained with antibodies to AC3 (red) and GFAP (green). Three cells are GFAP-positive (green), signifying that they are astrocytes. A fourth cell is AC3-positive, signifying that it is dying by apoptosis, but GFAP does not co-label with AC3 in this cell, signifying that it is not an astrocyte. Bar in (A) = 50 μ m for (A–C) and 30 μ m for (D).

marked dying neurones. Recently, we made the same observation in fetal NHP brains exposed to isoflurane.^{23 24} Therefore, in the fetal NHP brain, it appears that fractin staining is a selective tool for marking glial cells that succumb to apoptosis after anaesthesia exposure.

The majority of cells in the WM are either astrocytes or OLs. Therefore, we performed an immunofluorescent double staining experiment in which AC3-stained sections were also stained with antibodies against GFAP (marker for astrocytes), and found that the AC3-positive profiles did not co-label for GFAP (Fig. 4D), thus were not astrocytes. We conducted additional double staining experiments and, consistent with our previously reported findings in isoflurane-exposed fetal^{23 24} or neonatal²² NHP brains, we found that AC3-positive profiles in the WM did not co-label for NeuN, PDGFR α , or Iba1, signifying that the vulnerable WM cells were not neurones, OL progenitors or microglial cells (data not shown).

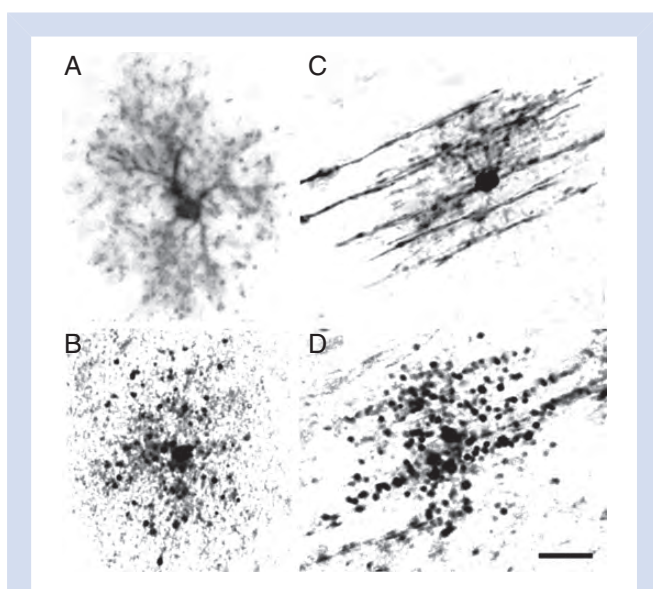


Fig 5 Histological appearance of MBP-stained OLs. (A) The appearance of a typical premyelinating OL in the *rostral* WM of a control fetal NHP brain that stains with antibodies to MBP because it has accumulated MBP in its cytoplasm and processes in preparation for myelinating axons. This cell is in a state of readiness, but has not yet become engaged in myelination. In propofol-exposed brains there were numerous MBP-positive premyelinating OLs that appeared to be dying. The typical appearance of these MBP-positive premyelinating OLs in an advanced stage of degeneration is depicted in (B). (C) From a *mid-rostrocaudal* section where myelination is occurring, this micrograph illustrates the appearance of an MBP-positive OL that is engaged in early myelination. MBP antibodies stain the cell body and processes of the OL, and also stain multiple myelin sheaths with which its processes are in continuity. (D) When an OL succumbs to cell death while it is engaged in early myelination, MBP staining reveals that the degeneration products cluster in the central compartment (remains of the cell body) and line up in a linear pattern conforming to the configuration of the patch of axons it was myelinating. Scale bar in (D)=15 μ m and pertains to all panels.

Based on these findings we explored the possibility that the degenerating cells in the fetal NHP WM are differentiated OLs that have matured beyond the stage of OL progenitors. We used MBP, a specific marker for myelin, and therefore for OLs that are becoming competent to myelinate axons.^{26 27 29} In sections cut through the frontal cortex at or rostral to the septum, MBP staining revealed no evidence for myelination, but at this level there were numerous MBP-positive OLs that, judged by their MBP content, were in a state of readiness to begin the myelination process. These premyelinating OLs in control brains presented a dense display of web-like radial processes, and they had just enough MBP in their soma and processes to allow the full morphology of the cell to be visualized (Fig. 5A). In the propofol-exposed brains, many of these premyelinating OLs showed signs of degeneration. In the early stages the signs were subtle, but in more advanced stages, the cell body was condensed and shrunken and the processes were severely fragmented (Fig. 5B), giving these profiles an appearance similar to those stained with cell death markers, AC3, silver or fractin (compare Fig. 5B with Fig. 4A–C). These findings confirm that OLs, while they are in a premyelinating maturational stage, and before they have begun to myelinate axons, are susceptible to the apoptogenic action of propofol.

To gain further insight into the size of the cell population at risk of dying by apoptosis after propofol exposure at G120 of fetal development, we conducted immunofluorescent double staining experiments using MBP as a marker of premyelinating OLs and fractin as a marker of cells undergoing degeneration. This staining was performed on rostral sections where all of the cells that stain positive for MBP are premyelinating OLs. Figure 6 presents a section from the rostral centrum semiovale where there are frequent cell bodies that stain positive for MBP (Fig. 6). Surprisingly, all of the profiles that are MBP-positive in Figure 6A show varying degrees of positivity for fractin in Figure 6B and C. We also observed an inverse relationship between the intensity of MBP staining and intensity of fractin staining (i.e. cells revealing the most intense fractin staining tend to show less intense MBP staining, and vice versa). The most likely explanation for this is that it takes time, after the MBP-positive premyelinating OL has committed to cell death, for activated caspases to flood the cell and generate significant concentrations of fractin by proteolytic breakdown of actin. During that time, the MBP content of the cell becomes altered by the degenerative process, which weakens its antigenicity. These double staining results suggest that a very high percentage of MBP-positive OLs that are in a premyelinating state at the time of anaesthesia exposure sustain injury and possibly go on to die.

We also analysed sections from the same G120 fetal brains at the mid-rostrocaudal and the cerebellar-brainstem levels. At a mid-rostrocaudal level, MBP staining revealed evidence for active myelination in several WM regions including the centrum semi-ovale (CSO), internal capsule (IC) and globus pallidus. MBP staining provided evidence that early myelination proceeds in steps beginning with single MBP-positive OLs contacting multiple axons and transferring MBP to them, allowing

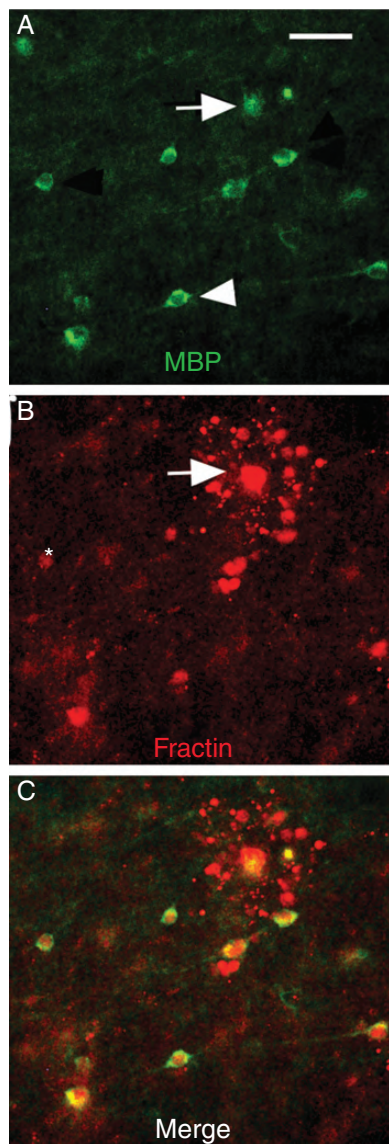


Fig 6 Immunofluorescent double staining of premyelinating OLs with antibodies to MBP and fractin. The micrograph depicts cell degeneration in the rostral CSO WM of a propofol-exposed NHP fetal brain. (A) MBP (green) stains, with varying degrees of intensity, about nine cellular profiles (one example marked by arrowhead). (B) Fractin antibodies also mark the same profiles with varying degrees of intensity. One of the fractin-positive profiles (arrow in A and B) is in an advanced stage of degeneration, as evidenced by the starburst halo of fractin-positive degeneration products surrounding the profile that represents dense accumulation of fractin in the centre of the disintegrating cell body. The remaining fractin-positive cells are in earlier stages and have less fractin-positive debris in their cytoplasm. The merged image in (C) reveals that MBP and fractin co-localize in all of the profiles that were MBP-positive in (A), but the cell that has the greatest display of fractin positivity (arrow in A and B) has relatively faint MBP positivity (arrow in A), suggesting that the degenerative process may tend to extinguish MBP positivity. Profiles in (B) that are only faintly stained with fractin (asterisk) are in an early stage of injury and therefore have generated only small amounts of fractin. Scale bar in (A) = 25 μm for all panels.

them to be visualized as a patch of MBP-positive axonal segments (Fig. 5c). MBP staining also revealed that some of these myelinating OLs in propofol-exposed brains were undergoing degeneration, and the degeneration products were lined up in linear streaks conforming to the layout of the axonal patch that the disintegrated OL was myelinating at the time of cell death (Fig. 5d). Double staining experiments determined that AC3-positive profiles were typically also MBP-positive (Fig. 7A–C), and DAPI counterstaining revealed an abnormal nuclear chromatin pattern indicative of apoptotic cell death (Fig. 7D).

At the caudal cerebellar/brainstem level, ascending WM tracts were already heavily myelinated at G120 and MBP staining provided an excellent means of visualizing these myelinated pathways. However, while distinctively staining the dense myelin sheet layers, MBP did not stain the cell bodies of the associated OLs. Double staining experiments in propofol-exposed brains using MBP, AC3 and fractin provided evidence for many cell bodies that could not be detected by MBP staining but were strongly positive for AC3 or fractin (cell death markers) amidst a dense bed of MBP-positive myelin sheaths (Fig. 8A and B). These cells presumably are mature OLs, the cell bodies of which do not stain positive for MBP, probably because they have transferred all of their MBP content

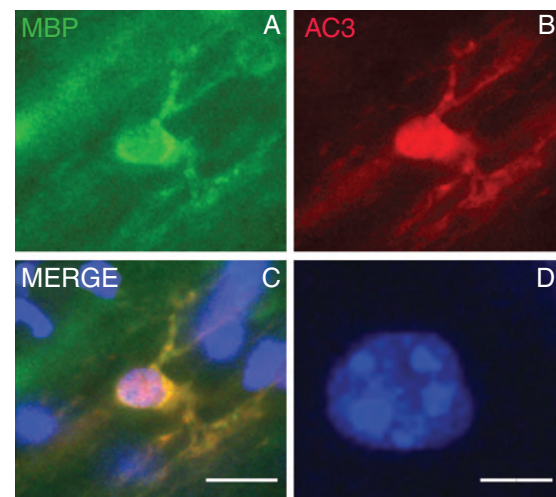


Fig 7 Immunofluorescent double staining with antibodies to MBP and AC3. (A) A myelinating OL in a propofol-exposed fetal NHP brain stained with the MBP-antibody (green). The cell body is densely positive for MBP and its MBP-positive processes are in contact with axons that it is myelinating. (B) This same cell co-labels for AC3 including its processes, which is confirmed by the merged image in (C). MBP positivity of the cell body signifies that this is an OL; contact and confluence of its processes with MBP-positive myelin sheaths confirms that it is engaged in myelinating axons; AC3 positivity signifies that this OL is undergoing apoptotic degeneration. DAPI counterstaining (D, blue colour) shows at increased magnification that the nucleus of this cell has a pattern of nuclear chromatin clumping that proves apoptotic cell death. Scale bar in (C) = 15 μm for (A–C); scale bar in (D) = 5 μm .

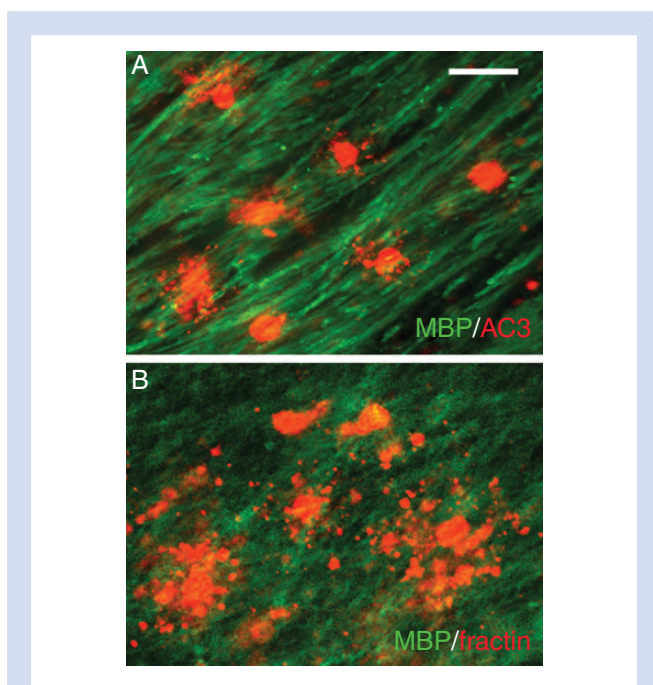


Fig 8 Immunofluorescent double staining with antibodies to MBP and AC3 (A) or MBP and fractin (B) of degenerating OLs in a heavily myelinated caudal WM pathway (cerebellar peduncle) from a propofol-exposed fetal NHP brain. MBP staining in both of these panels reveals that myelinated axonal bundles are strongly immunoreactive for MBP antibodies, but there are no MBP-positive cell bodies. Both cell death markers (AC3 and fractin) vividly stain dying cells that are intermingling with the MBP-positive fibre bundles, but none of these dying cell bodies are immunoreactive for MBP. Scale bar in (A) = 15 μm for both panels.

to myelin sheaths, and then have ceased storing MBP in their cell bodies. However, proving the identity of these degenerating cells in densely myelinated pathways is problematic. We demonstrated recently²² that in isoflurane-exposed neonatal NHP brains, morphologically similar cells in the same region stained intensely for AC3, but faintly or not at all for Olig 2 or corpus callosum (CC)-1, which are currently recognized as markers of mature OLs.^{30–32} Faint staining for these mature OL markers was present if the cell was in a very early stage of degeneration, and no staining was observed if the cell showed signs of more advanced degeneration, suggesting that when these cells are degenerating they rapidly lose immunoreactivity for these markers.

Response of the neonatal NHP brain to propofol

The P6 animals randomized to receive propofol ($n=4$; mean age 6 days; range 4–6) had a body weight of 411–640 g on the day of the experiment and were similar to the animals comprising the control group ($n=5$; mean age 6 days; range 4–7; body weight 430–546 g). Propofol anaesthesia was well tolerated by all infant animals and vital signs remained within normal limits throughout the experimental period. Anaesthetized animals were weaned from the ventilator within 15 min, and the trachea was extubated within 75 min after

discontinuation of propofol. There were no adverse effects of propofol anaesthesia observed in the neonatal cohort. Supplementary Table S3 summarizes baseline variables of both the anaesthetized and the non-anaesthetized ('control') groups, and confirms that the physiological response to propofol was within the normal species-specific range. No complications occurred during *in-vivo* tissue fixation.

Quantitative findings

Quantitative evaluation of AC3-stained sections from the neonatal brains exposed to propofol ($n=4$) revealed that the mean (SEM) number of all AC3-positive profiles (neurons+glia) per brain was $12.01 (2.4) \times 10^5$, and in the control brains ($n=5$) was $3.17 (0.85) \times 10^5$ (Fig. 1). Hence, there was a 3.8-fold increase in the number of apoptotic profiles in the propofol-exposed brains compared with the brains from drug-naive controls. The difference in the mean number of apoptotic profiles between the propofol and control groups was 8.8×10^5 (95% CI, $14.3 - 3.3 \times 10^5$, $P=0.007$). In the neonatal NHP brains exposed to propofol, the mean number of dying (AC3-positive) neurons was approximately equal to the mean number of AC3-positive OLs (6.3×10^5 for neurons and 5.7×10^5 for OLs).

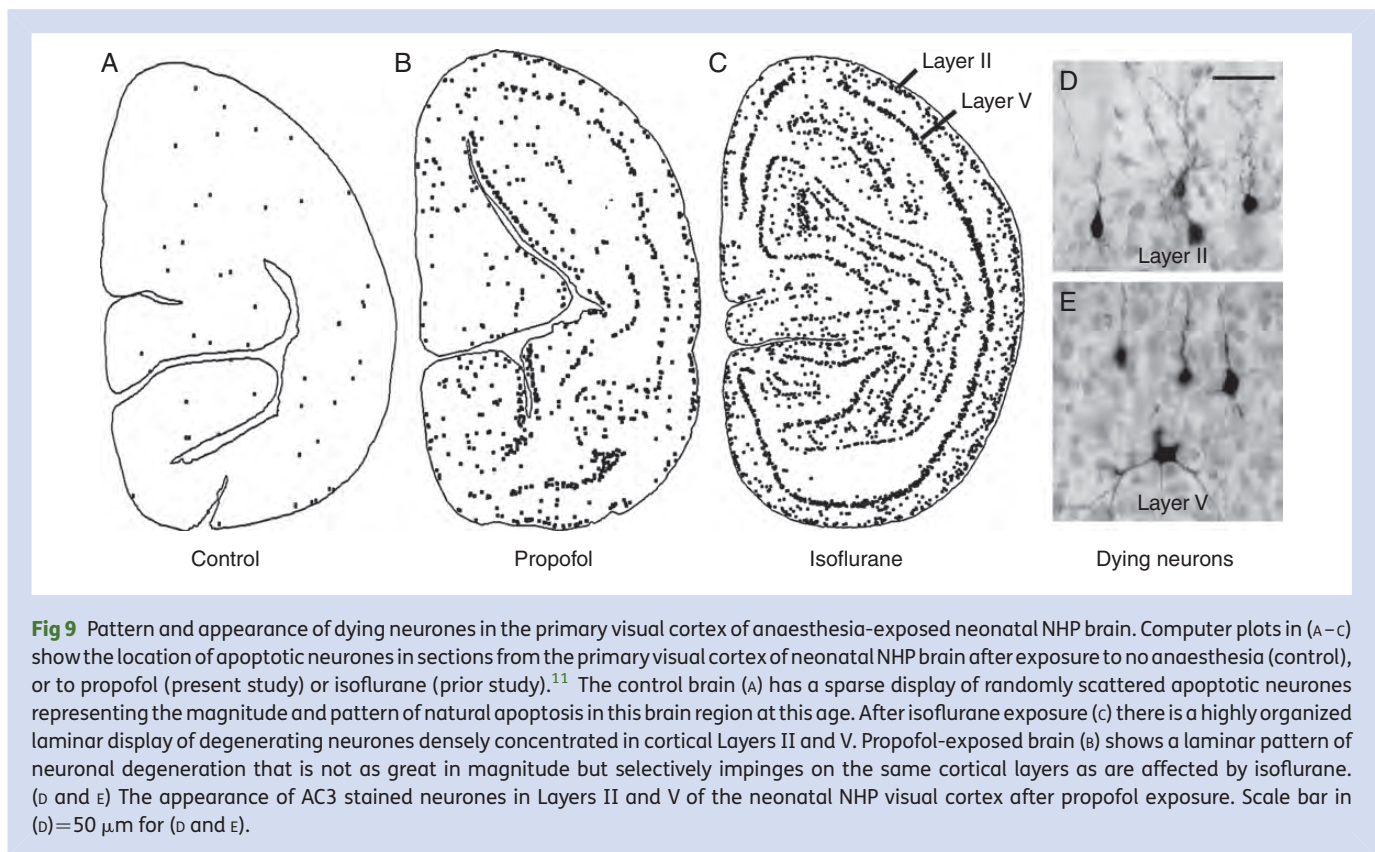
Descriptive histopathology

The regional distribution of neurons undergoing acute apoptotic degeneration in the propofol-exposed P6 neonatal NHP brain, as assessed by AC3 staining, was different than was observed in the propofol-exposed fetal brains. The primary differences were that neurons in caudal brain regions, including the cerebellum and inferior colliculus, were relatively spared, and in the forebrain the most robust neuronal cell death response was in the somatosensory and auditory association centres of the parietal and temporal lobes, respectively, and in the primary visual cortex of the occipital lobe (Fig. 9). In these neocortical brain regions, the pattern of neuronal degeneration was distinctly laminar with Layers II and IV in the somatosensory and auditory cortices, and Layers II and V in the primary visual cortex, most prominently involved. This pattern of neuronal degeneration is very similar to the pattern we have described¹¹ in the neonatal NHP brain after isoflurane anaesthesia (Fig. 9).

Degenerating glial profiles visualized by AC3 staining in the propofol-exposed neonatal brains were distributed diffusely throughout the WM and were abundantly present in areas where early myelination was ongoing, and also in areas of relatively mature myelination. The WM profiles stained by AC3 were identical in morphological appearance to those in the fetal brains, and these profiles were also readily detected by both silver and fractin staining (data not shown).

Discussion

Our findings demonstrate that exposure of fetal or neonatal NHP brain to propofol anaesthesia for 5 h is sufficient to cause a robust apoptotic cell death response affecting both neurons and glia. Apoptotic death of neurons, glia, or both



has been described previously in the developing NHP brain^{8–12, 22–24} after exposure to isoflurane or ketamine, but this is the first report describing this same cell death response affecting both neurones and glia in the developing NHP brain after exposure to propofol. The glial cell type selectively affected in both the neonatal and fetal brain by isoflurane (prior studies)^{22–24} or propofol (present study) is in the OL lineage, and onset of vulnerability occurs at a maturational stage when the OL is beginning to generate MBP in preparation for myelinating axons. OL progenitor stages were not affected, nor were other glial cell types. The overall number of apoptotic profiles (neurones+OLs) in propofol-exposed fetal and neonatal brains, respectively, was 2.4 and 3.8 times greater than in the corresponding drug-naïve control brains. Of the total number of degenerating cells in propofol-exposed brains of either fetal or neonatal age, approximately half were neurones and half OLs.

The pattern of neuronal degeneration induced by propofol in neonatal NHP brain was different from that induced in fetal brain. In neonatal brain, a laminar pattern of neuronal degeneration was strikingly evident in specific layers and regions of the cerebral cortex (Layers II and IV of the auditory and somatosensory association cortices in the temporal and parietal lobes, and Layers II and V of the primary visual cortex in the occipital lobe). Other cortical and subcortical regions in the neonate were affected but not as severely. In addition, there was a tendency for rostral brain regions to be more affected, and caudal regions, for example the cerebellum, to be spared. In contrast, in the fetal brain propofol induced pronounced degeneration in caudal brain regions, especially the

cerebellum and inferior colliculus, and in rostral brain regions subcortical neuronal populations (caudate, putamen, nucleus accumbens, and amygdala, thalamus) were more severely affected than neurones in the cerebral cortex. The pattern observed here for propofol in both fetal and neonatal brain closely resembles that described previously^{22–24} for isoflurane. This pattern is different, especially in neonatal brain, from that described for ketamine,¹² in that ketamine does not show a predilection for large numbers of degenerating neurones in specific layers of the visual, auditory and somatosensory cortices. These differences could reflect differences in the receptor specificities of these agents, in that isoflurane and propofol act predominantly at γ -aminobutyric acid type A (GABA_A) receptors and ketamine at *N*-methyl-D-aspartate glutamate receptors.

The apoptogenic action of anaesthetic drugs on glial cells appears to target a single glial cell type, the OL, with onset of vulnerability coinciding with the stage when the OL is beginning to accumulate MBP. OLs are responsible for the generation and maintenance of myelin that ensheathes axons and enables neurones to function effectively. MBP is a building block of myelin that comprises 30% of the myelin sheath.²⁷ Death of OLs at a time when they are just beginning to generate MBP is a pathological phenomenon that potentially could have adverse effects that might add to, or even potentiate, the functional consequences of propofol-induced neuronal death. Our present findings in both fetal and neonatal NHP brain indicate that onset of vulnerability to the apoptogenic action of propofol corresponds to the time when premyelinating OLs

are beginning to generate constituents of myelin, which in the human developing brain may occur early in the second trimester.^{33 34} Our findings indicate that vulnerability does not cease until some undetermined time after axonal pathways are relatively well myelinated. In the human, myelination continues in some brain regions, for example, the hippocampus, until late adolescence.³⁵ It will be important in future NHP research to determine at what prenatal age the window of vulnerability opens for anaesthesia-induced apoptosis of OLs and of neurones, and at what postnatal age it closes.

Although the patterns of degeneration induced by propofol and isoflurane are similar, the toxic impact of isoflurane is substantially greater than the impact of propofol, especially in neonatal brain. Subtracting the total mean number of apoptotic profiles (neurones+OLs) per control brain from the total mean number per anaesthesia-exposed brain yields the total mean number of dying cells that can be attributed to anaesthesia exposure. That number for the neonatal NHP brain exposed to isoflurane (prior study)¹¹ is 37×10^5 , and for the neonatal NHP brain exposed to propofol (present study) is 8.8×10^5 . This indicates that when neonatal NHP brain is exposed for the same duration to a surgical plane of isoflurane or propofol anaesthesia, the toxic impact of isoflurane is in the range of four times greater than that of propofol. While an important purpose of studying the effects of anaesthetic drugs on the developing NHP brain is to determine whether some anaesthetic agents might be safer than others, a caveat in interpreting our present findings is that they pertain to a small number of animals (4–5 per treatment condition). Thus, our findings are of heuristic value for guiding future research, but for guiding clinical practice it would be valuable to confirm these findings with a larger number of NHP subjects.

Supplementary material

Supplementary material is available at *British Journal of Anaesthesia* online.

Authors' contributions

C.C. and K.D. conducted the histological and immunohistochemical studies. G.D. and L.M. directed the time-mated breeding and the veterinary care of the animals. J.O. together with A.B., as co-principal investigators, directed the work, data analysis and interpretation, and manuscript preparation. A.B. designed and conducted all animal experiments. All authors contributed to the writing of the manuscript.

Declaration of interest

None declared.

Funding

This work was supported in part by the National Institutes of Health, Bethesda, MD, USA; grants HD052664, HD37100, and HD062171; and by DA 05072 and 8P51OD011092 for the operation of the Oregon National Primate Research Center.

References

- 1 Ikonomidou C, Bosch F, Miksa M, et al. Blockade of NMDA receptors and apoptotic neurodegeneration in the developing brain. *Science* 1999; **283**: 70–4
- 2 Jevtovic-Todorovic V, Hartman RE, Izumi Y, et al. Early exposure to common anesthetic agents causes widespread neurodegeneration in the developing rat brain and persistent learning deficits. *J Neurosci* 2003; **23**: 876–82
- 3 Rizzi S, Carter LB, Ori C, Jevtovic-Todorovic V. Clinical anesthesia causes permanent damage to the fetal guinea pig brain. *Brain Pathol* 2008; **18**: 198–210
- 4 Satomoto M, Satoh Y, Terui K, et al. Neonatal exposure to sevoflurane induces abnormal social behaviors and deficits in fear conditioning in mice. *Anesthesiology* 2009; **110**: 628–37
- 5 Fredriksson A, Archer T, Alm H, Gordh T, Eriksson P. Neurofunctional deficits and potentiated apoptosis by neonatal NMDA antagonist administration. *Behav Brain Res* 2004; **153**: 367–76
- 6 Istaphanous GK, Howard J, Nan X, et al. Comparison of the neuro-apoptotic properties of equipotent anesthetic concentrations of desflurane, isoflurane, or sevoflurane in neonatal mice. *Anesthesiology* 2011; **114**: 578–87
- 7 Cattano D, Young C, Olney JW. Sub-anesthetic doses of propofol induce neuroapoptosis in the infant mouse brain. *Anesth Analg* 2008; **106**: 1712–4
- 8 Slikker W Jr, Zou X, Hotchkiss CE, et al. Ketamine-induced neuronal cell death in the perinatal rhesus monkey. *Toxicol Sci* 2007; **98**: 145–58
- 9 Zou X, Patterson TA, Divine RL, et al. Prolonged exposure to ketamine increases neurodegeneration in the developing monkey brain. *Int J Dev Neurosci* 2009; **27**: 727–31
- 10 Zou X, Liu F, Zhang X, et al. Inhalation anesthetic-induced neuronal damage in the developing rhesus monkey. *Neurotoxicol Teratol* 2011; **33**: 592–7
- 11 Brambrink AM, Evers AS, Avidan MS, et al. Isoflurane-induced neuroapoptosis in the neonatal rhesus macaque brain. *Anesthesiology* 2010; **112**: 834–41
- 12 Brambrink AM, Evers AS, Avidan MS, et al. Ketamine-induced neuroapoptosis in the fetal and neonatal rhesus macaque brain. *Anesthesiology* 2012; **116**: 372–84
- 13 Sanders RD, Xu J, Shu Y, et al. Dexmedetomidine attenuates isoflurane-induced neurocognitive impairment in neonatal rats. *Anesthesiology* 2009; **110**: 1077–85
- 14 Paule MG, Li M, Allen RR, et al. Ketamine anesthesia during the first week of life can cause long-lasting cognitive deficits in rhesus monkeys. *Neurotoxicol Teratol* 2011; **33**: 220–30
- 15 DiMaggio C, Sun LS, Kakavouli A, Burne MW, Li G. A retrospective cohort study of the association of anesthesia and hernia repair surgery with behavioral and developmental disorders in young children. *J Neurosurg Anesthesiol* 2009; **4**: 286–91
- 16 DiMaggio C, Sun L, Li G. Early childhood exposure to anesthesia and risk of developmental and behavioral disorders in a sibling birth cohort. *Anesth Analg* 2011; **113**: 1143–51
- 17 Wilder RT, Flick RP, Sprung J, et al. Early exposure to anesthesia and learning disabilities in a population-based birth cohort. *Anesthesiology* 2009; **110**: 796–804
- 18 Block RI, Thomas JJ, Bayman EO, Choi JW, Kimble KK, Todd MM. Are anesthesia and surgery during infancy associated with altered academic performance during childhood? *Anesthesiology* 2012; **117**: 494–503

- 19 Flick RP, Katusic SK, Colligan RC, et al. Cognitive and behavioral outcomes after early exposure to anesthesia and surgery. *Pediatrics* 2011; **128**: e1053–61
- 20 Sprung J, Flick RP, Katusic SK, et al. Attention-deficit/hyperactivity disorder after early exposure to procedures requiring general anesthesia. *Mayo Clin Proc* 2012; **87**: 120–9
- 21 Ing C, DiMaggio C, Whitehouse A, et al. Long-term differences in language and cognitive function after childhood exposure to anesthesia. *Pediatrics* 2012; **130**: e476–85
- 22 Brambrink AM, Back SA, Riddle A, et al. Isoflurane-induced apoptosis of oligodendrocytes in the neonatal primate brain. *Ann Neurol* 2012; **72**: 525–35
- 23 Brambrink AM, Dikranian K, Evers AS, Creeley CE, Olney JW. Isoflurane-induced apoptosis of neurons and oligodendrocytes in the fetal rhesus macaque brain. *American Society of Anesthesiologists. Annual Meeting Program Webpage* 2012; LBB10 (Late Breaking abstracts)
- 24 Creeley CE, Dikranian KT, Back SA, Dissen GA, Olney JW, Brambrink AM. Isoflurane-induced apoptosis of neurons and oligodendrocytes in the fetal Rhesus macaque brain. *Anesthesiology* (accepted for publication) 2013
- 25 Schulz R, Vogel T, Mashima T, Tsuruo T, Krieglstein K. Involvement of fractin in TGF-beta-induced apoptosis in oligodendroglial progenitor cells. *Glia* 2009; **57**: 1619–29
- 26 Butt AM, Berry M. Oligodendrocytes and the control of myelination *in vivo*: New insights from the rat anterior medullary velum. *J Neurosci Res* 2000; **59**: 477–88
- 27 Baumann N, Pham-Dinh D. Biology of oligodendrocyte and myelin in the mammalian central nervous system. *Physiol Rev* 2001; **81**: 871–927
- 28 Farber NB, Creeley CE, Olney JW. Alcohol-induced neuroapoptosis in the fetal macaque brain. *Neurobiol Dis* 2010; **40**: 200–6
- 29 Pfeiffer SE, Warrington AE, Bansal R. The oligodendrocyte and its many cellular processes. *Trends Cell Biol* 1993; **3**: 191–7
- 30 Kitada M, Rowitch DH. Transcription factor co-expression patterns indicate heterogeneity of oligodendroglial subpopulations in the adult spinal cord. *Glia* 2006; **54**: 35–46
- 31 Sohn J, Natale J, Chew LJ, et al. Identification of Sox17 as a transcription factor that regulates oligodendrocyte development. *J Neurosci* 2006; **26**: 9722–35
- 32 Koenning M, Jackson S, Hay CM, et al. Myelin gene regulatory factor is required for maintenance of myelin and mature oligodendrocyte identity in the adult CNS. *J Neurosci* 2012; **32**: 12528–42
- 33 Jakovcevski I, Mo Z, Zecevic N. Down-regulation of the axonal polysialic acid-neural cell adhesion molecule expression coincides with the onset of myelination in the human fetal forebrain. *Neuroscience* 2007; **149**: 328–37
- 34 Jakovcevski I, Filipovic R, Mo Z, Rakic S, Zecevic N. Oligodendrocyte development and the onset of myelination in the human fetal brain. *Front Neuroanat* 2009; **3**: 5
- 35 Abraham H, Vincze A, Ilja J, et al. Myelination in the human hippocampal formation from midgestation to adulthood. *Int J Dev Neurosci* 2010; **28**: 401–10

Handling editor: H. C. Hemmings